PII: S0032-3861(97)10115-X

Polymer Vol. 39 No. 14, pp. 3099–3108, 1998

0032-3861/98/$19.00+0.00

The ordering of semi-crystalline PS-b-hPB copolymers at a PS/PE interface and their effects on interfacial strength

H. E. Hermes[a,*], **D. G. Bucknall**[b], **J. S. Higgins**[a] **and R. L. Scherrenberg**[c]
[a] *Department of Chemical Engineering and Chemical Technology, Imperial College, Prince Consort Road, London SW7 2BY, UK*
[b] *ISIS Facility, Rutherford Appleton Laboratory, Chilton, Didcot, Oxon OX11 0QX, UK*
[c] *DSM Research, P.O. Box 18, 6160 MD Geleen, The Netherlands*
(Received 25 July 1997)

The organisation and mechanical effectiveness of a series of polystyrene-block-hydrogenated polybutadiene (PS-b-hPB) diblock copolymers (where the hPB block is semicrystalline) when placed as thin layers between the immiscible polymers, polyethylene (PE) and polystyrene (PS), has been explored using neutron reflectivity, transmission electron microscopy and mechanical peel tests. For thin copolymer layers (expected to leave the interface unsaturated) the trend in variation of interfacial strength with copolymer molecular weight was found to be similar to that previously reported for amorphous copolymers. However, for thick layers (oversaturating the interface) the interfacial strength became in one case too large to separate the layers in the peel test. This may suggest a different mechanism for increasing interfacial strength when at least one of the copolymer blocks is crystallisable. © 1998 Elsevier Science Ltd. All rights reserved.

(Keywords: PS/PE interface; adhesion; compatibilisation)

INTRODUCTION

It is often stated that immiscible polymer blends have poor mechanical properties due to the poor adhesion between the blend components, and that improving the adhesion between the blend components will hence lead to improved mechanical properties. In this project, of which the results reported here are a part, the effects of a set of semi-crystalline PS-b-hPB diblock copolymers of various molecular weights on the bulk morphological and mechanical properties, as well as the interfacial properties of a PS/PE blend were investigated. The bulk properties and their relationship to the interfacial properties reported here are discussed elsewhere[1].

The effects of an A–B diblock copolymer on the properties of the interface between immiscible homopolymers A and B has been described theoretically by Shull and Kramer[2]. Their calculations suggest that because the junction between the copolymer blocks is constrained to the interface, only a small increase in the width of the region over which A and B segments mix occurs upon addition of copolymer to the interface. However, the blocks of the copolymer are shown to extend away from the interface into the homopolymers. Shull and Kramer suggest that it is this penetration of the block copolymer into the homopolymer phases, not the increase in segmental mixing, that must be primarily responsible for enhanced adhesion between immiscible polymers observed on addition of copolymers.

In contrast to the predictions of Shull and Kramer, experimental results tend to show a significant increase in interfacial width when a copolymer is added to an immiscible blend. For example, Russell and co-workers find, using NR, that above a certain copolymer coverage at the interface, further addition of a PS-b-PMMA diblock copolymer to the interface between PS and PMMA leads to an apparent dramatic broadening of the interface[3]. When the thickness of the copolymer film placed between the PS and PMMA is less than half the period of the lamellar microdomain morphology of the copolymer in the bulk, 0.5 L_0, they observe only a moderate increase in the interfacial width i.e., similar to that predicted by Shull and Kramer. Russell and co-workers suggest that when the copolymer layer thickness exceeds 0.5 L_0, the interface becomes saturated with copolymer and that the apparent interfacial thicknesses measured for copolymer layers thicker than this are not likely to be real. By investigating the off-specular scattering they suggest two possible reasons for the apparent increase in interfacial width. Firstly, they argue that the presence of the diblock copolymer at the interface will reduce the interfacial tension between the PMMA and PS and that a point will eventually be reached where the interfacial tension tends to zero. At this point energy will no longer be gained by maintaining a planar interface and marked curvature of the interface may occur. Since measurements of specular reflectivity represent the variation in the scattering length density normal to the film surface averaged over the coherence length of the neutrons (≈ 1 μm), any curvature at the interface that occurs over distance scales smaller than this appear as interfacial broadening. As an alternative explanation they suggest that once the interface is saturated, addition of further copolymer may result in the formation of micelles at the interface. Again the specular measurements would average over the micelles formed and give the appearance that the interface has broadened significantly.

---

[*] To whom correspondence should be addressed

The literature on the effects of diblock copolymers on the interfacial strength between immiscible homopolymers is dominated by the work of Brown, Creton, Kramer and co-workers predominantly on glassy–glassy systems[4–13]. Using an asymmetric double cantilever beam test, they found that the principle variables governing the interfacial strength of diblock copolymer-modified interfaces are the areal chain density, Σ, of the block copolymer at the interface and the molecular weights of the copolymer blocks. From their results they have suggested a fracture mechanism map for copolymer reinforced interfaces which divides the fracture behaviour into three regimes.

In regime I, applicable for copolymers with high degrees of polymerisation i.e., $M_w \gg$ molecular weight of entanglement, M_e, two failure mechanisms are possible. For copolymer areal densities less than a critical value, Σ_c, chain scission of the block copolymer chains near the junction between the two blocks is expected to occur. This is because at these areal densities the total stress required to break the copolymer chains, σ_{scission}, is less than the crazing stress of the homopolymers, σ_{craze}. At higher areal densities of copolymer, i.e., $\Sigma > \Sigma_c$, σ_{scission} exceeds σ_{craze}, and it is expected that the interface will fail by crazing in the homopolymer with the lowest crazing stress. It has been found that throughout this regime, the strength of the interface is proportional to Σ^2.

In regime II, which is applicable to copolymers with intermediate degrees of polymerisation, a transition from chain pullout to crazing is expected to occur. For the PS/PVP system, Washiyama and co-workers[8] found that this transition occurred at 0.04 chains/nm^2.

Regime III applies when the degree of polymerisation of the copolymer is low i.e., $M_w < M_e$. In this regime, $\sigma_{\text{pullout}} < \sigma_{\text{craze}}$ over the entire range of areal densities less than the saturation areal density, Σ_{sat}, and hence chain pull out is the only failure mechanism expected. Creton and co-workers found that for $\Sigma < \Sigma_{\text{sat}}$, the strength of the interface is proportional to Σ in this regime[7]. Washiyama and co-workers confirmed this and found that for a constant degree of polymerisation and areal density, the friction coefficient between the copolymer block being pulled out and the corresponding homopolymer determines the strength of the interface in this regime[13].

If the copolymer areal density exceeds Σ_{sat}, the interface becomes saturated with copolymer. Additional copolymer chains can then no longer organise as a brush at the interface, but must form micelles, lamellae or some other structure at the interface. Washiyama and co-workers found that addition of more block copolymer than needed to saturate the interface may produce secondary interfaces which are weaker than the original saturated homopolymer one[11]. They found that this was the case for symmetrical diblock copolymers which formed lamellae at the interface when $\Sigma > \Sigma_{\text{sat}}$. However, for asymmetrical diblock copolymers which formed spherical micelles on one side of the interface at high copolymer areal densities, they found that the interfacial strength remained constant at the maximum value attained when $\Sigma \approx \Sigma_{\text{sat}}$.

Brown and co-workers have also investigated the effect of PS-b-PI (polyisoprene) diblock copolymers on the interface between PS and cross-linked PI using a peel test and the so-called JKR test, in which an elastic spherical cap (the cross-linked PI) is pushed into contact with either a second spherical cap or a flat substrate (the PS). The change in contact radius with time can then be used to give a value of interfacial strength[14–16]. As expected for elastomers, the interfacial toughness was found to be dependent upon crack speed. The areal density and copolymer block length were also found to affect interfacial strength. For one high molecular weight copolymer, the length of time the copolymer coated PS strip was in contact with the PI prior to testing was also found to have an effect. It was proposed that this was due to the slower diffusion of the higher molecular weight PI block into the PI matrix, compared with low molecular weight blocks.

In this paper, the organisation of a series of semi-crystalline PS-b-hPB copolymers of differing molecular weights when placed as thin layers at the interface between the immiscible homopolymers PS and PE, and their effect on the mechanical strength of the interface are discussed. To study these effects we have used peel tests, neutron reflectivity and transmission electron microscopy.

EXPERIMENTAL

Polymer characteristics

The molecular characteristics of the polymers used in these investigations are shown in *Tables 1* and *2*. All the homopolymers and copolymers were provided by DSM Research, The Netherlands, except for the deuterated PS, which was prepared by Professor R.W. Richards' group at the University of Durham. The hydrogenous PS used is a general purpose, industrial polymer (Shell N7000). The PE is a low modulus research grade, similar to that described by Deblieck and co-workers[17]. The copolymers were prepared by sequential anionic polymerisation and used as supplied. GPC showed that the copolymers contained a small percentage of homopolymer PS. For the majority of copolymers, the homo-polystyrene content (based on the relative areas of the peaks in the GPC curves) was found to be less than 5%. However, copolymer 101hPB contained as much as 26% homo-polystyrene.

Neutron reflectivity

The technique of neutron reflectivity (NR) allows the determination of the composition profile of a sample normal to its surface. It provides detailed information about layer thickness, density and interfacial profile of the sample. Typically, NR has a resolution normal to the surface of 0.2 nm at 100 nm depth[18] and is capable of resolving the

Table 1 Homopolymers used in these investigations

Polymer	M_w	M_n
PS	278 300	104 800
PSd8	190 000	176 800
PE	43 700[a]	7800[a]

[a] GPC values: LDPE equivalent molecular weights

Table 2 Diblock copolymers used in these investigations

	PS block (× 1000)		overall(× 1000)		
	M_w	M_n	M_w[a]	M_w[b]	M_n[a]
8hPB	8.2	7.9	36	37	33
21hPB	21	20	53	54	49
42hPB	42	41	120	123	110
101hPB	101	97	210	214	170
10d8hPB	9.9	9.6	26	26.6	23
96d8hPB	96	91	250	255.7	210

[a] Before hydrogenation

[b] Assuming 100% hydrogenation of double bonds

movement of chain segments across the interface between two polymer layers[19]. No information is obtained about the lateral structure because the measured reflectivity is an average obtained over a large area of illumination. The theory behind NR and its use to study polymer–polymer interfaces has recently been reviewed[20].

The basis of an NR experiment is to measure the specular reflection as a function of the wave vector transfer, **Q**, perpendicular to the reflecting surface ($\mathbf{Q} = (4\pi/\lambda)\sin(\theta/2)$ where λ = neutron wavelength, θ = angle of incidence). Samples prepared for NR need to be flat enough to minimise the off-specular scattering of the sample, which is deleterious to the specular reflectivity. Typically, for the investigations of polymer–polymer interfaces such flat samples are prepared by spin coating thin polymer films from solution onto optically flat substrates such as silicon or quartz. However, below the crystalline melt temperature the film surface of crystalline polymers, such as PE, are macroscopically rough, which leads to a loss of specular reflection. Heating samples above the crystalline melt point removes the crystallinity of the films but has been shown not to produce meaningful reflectivity profiles[21]. This is due to persisting long-range waviness. To overcome these problems the cell illustrated schematically in *Figure 1* was developed. This has been described in more detail elsewhere[22].

Reflectivity data obtained from a NR experiment cannot be directly translated into a scattering length density, $\rho_s(d)$, profile (from which the composition profile can be deduced). This is because there is a loss of phase information incurred due to the square term in the reflectivity coefficients[20]. Instead, NR data are usually analysed by proposing models for $\rho_s(d)$ and using these to calculate the reflectivity, which can then be compared with the experimental profile. By varying the parameters of the model the differences between the experimental and calculated reflectivity profiles can be minimised. To achieve this we have used a combination of maximum entropy fitting and model fitting using matrix formalism methods[23]. Maximum entropy fitting methods have an added advantage in that they make very few initial assumptions about the sample (i.e., it is almost a model free fitting procedure). The maximum entropy fitting method of Sivia and co-workers has been used here[24]. The models obtained from the maximum entropy method were checked for physical meaningfulness and then refined using standard matrix model fitting.

The results from model fitting alone must be treated with caution as they are generally by no means unique[25]. Complementary data from such techniques as TEM and secondary ion mass spectroscopy can be used to reduce the number of unknown model parameters. Unfortunately, for many of the specimens studied for this work complementary evidence was not available. Comparison of the models obtained from fits of similar samples with varying contrast, however, allowed determination of the structure of the specimens with a fairly good degree of confidence.

For these NR experiments tri-layer samples of PE, copolymer and PS were investigated in the specially developed temperature controlled cell, see *Figure 1*. The PS layer was spun cast from toluene directly onto the Si substrate. The bulk PE was pressed into the mould using a hot press at 150°C. After cooling the bulk PE layer, the copolymer was spun directly onto it from a warm toluene solution. No interdiffusion of the copolymer is expected, since PE is insoluble in toluene. After drying, these samples were carefully stored in the dark until required.

When assembled, the reflectivity cell was covered with a box and purged continually with nitrogen, thus maintaining a nitrogen blanket around the cell for the duration of the experiment. Each experiment including the neutron alignment procedure took approximately 4 h and was performed at a temperature of 150°C. The NR measurements were carried out on the CRISP and SURF time-of-flight (TOF) spectrometers at the ISIS Facility of the Rutherford Appleton Laboratory. The general layout of these instruments has been described in detail elsewhere[20]. Generally, three angles were measured per sample in order to provide the required **Q** range. The area of illumination and the instrumental resolution were kept constant for all the angles. Once the raw data had been collected they were reduced and normalised to reflectivity profiles as a function of **Q**. This involves correcting for the monitor and detector efficiencies, as well as for the cell transmissions. The data were then fitted as described above.

Peel tests

The relative interfacial strengths of the copolymer modified interfaces were determined by using a peel test with constant peel rate and sample dimensions. The properties of the peel arm (PE) and peel substrate (PS) were constant, since these were the same in all cases. The only variation in the samples was the molecular weight of the copolymer or the thickness of the copolymer layer placed between the PS and the PE. Therefore, the measured peel force can be used to rank the copolymers in terms of their effectiveness as interfacial strength improvers. However, because a considerable portion of the peel energy is dissipated as plastic bending of the peel arm, which will be influenced by the strength of the interface, there is no simple correlation between the measured peel force and the absolute strength of the interface, even if the characteristics of the peel arms and the peel rate are kept constant[26].

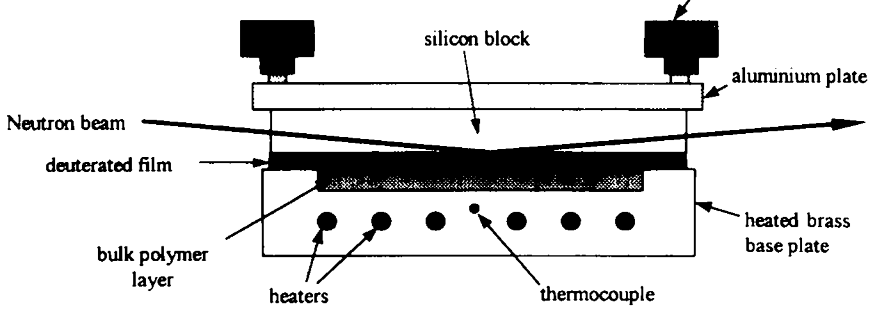

Figure 1 Schematic illustration of the melt cell used in the NR experiments

Peel test specimens were prepared by spin coating a thin layer (of the order of a few hundred Ångstroms thick) of copolymer onto the PE arm in the same manner employed in the preparation of the NR cell samples described above. The copolymer layer thickness could not be measured directly, but was estimated by comparison with known thicknesses of similar PS films prepared by spin casting. After spin coating, the PE slabs were placed in a vacuum oven at 40°C for several days to ensure that all the residual toluene had been removed. The PE slabs were then sandwiched to PS slabs with a piece of mylar film placed at one end of the sample between the two layers. This prevented adhesion at this point, and provided a starting point for the peel test. The sample was then placed in a mould which was approximately 0.1 mm thinner than its total uncompressed thickness. This was then placed in a hot press preheated to 150°C ± 4°C and heated for approximately 3 min without applying any pressure, followed by approximately 100 min with a load of 100 kN. The annealing time was measured from the point of applying the load. A standard annealing time of 100 min was used. The annealing temperature of 150°C was chosen not only because this temperature is above the melting point of the PE crystallites but it also allows direct comparison with the results from NR. After annealing under pressure for the required length of time, the heating was switched off and the heating plates water cooled. The sample temperature dropped to below the T_g of the PS within 5 min. After removal of the specimen from the press, they were stored in the dark until required for testing.

The 90° peel test arrangement (see *Figure 2*) was used because the PS is stiff at the testing temperature whilst the PE is flexible. The peel specimen was mounted on a slipless ball slide which was attached to the base plate of an Instron Model 1185 apparatus. This ensured that the angle between the PS base and the PE peel arm is maintained at 90°. The peel specimen was held rigidly in place by a single screw through one end of the specimen and a plate across the front of the PS slab, as shown in *Figure 2*. In addition, double-sided tape was used to stick the PS to the base plate to prevent the specimen bending. The peel arm was attached to the force measuring head via the clamp shown. The measurements were all carried out in a constant temperature room at 23°C. The experiment was performed by moving the base plate downwards at a constant speed of 1 mm/min and recording the resultant force on the force measuring head attached to the peel arm. For each specimen configuration four repeat specimens were measured.

Transmission electron microscopy

TEM micrographs were taken using a Philips CM200 TEM and an acceleration voltage of 120 kV. The blends were stained by placing specimens with pre-cut sectioning surfaces into a ruthenium tetroxide solution made from ruthenium (III) chloride hydrate and sodium hypochlorite for 48 h. The oxidation process was stopped by washing the specimens thoroughly in an excess of vitamin C solution, followed by rinsing with distilled water. Sections approximately 70 nm thick were then cut using a Reichert Ultracut-E microtome. Since crystalline structure was observed, the present staining technique clearly labels the PE phase in this system.

Differential scanning calorimetry

DSC measurements were performed on a Perkin-Elmer DSC-2. This had been modified to allow partial computer control and collection/analysis of the data. Samples weighing approximately 10–15 mg were used. These were sealed in standard aluminium pans. A scanning rate of 10°C/min was used. The same rate was used for both heating and cooling runs. Analysis of the curves was performed using the equipment analysis programs. The crystallisation temperature was taken as the peak value of the crystallisation curve.

RESULTS AND DISCUSSION

Organisation of the copolymer at the interface

Figures 3 and 4 illustrate TEM micrographs of sections ultramicrotomed from peel test samples which had been prepared by placing an approximately 60 nm thick copolymer film between PS and PE and subsequently annealing the 'sandwich' for 100 min at 150°C. Unfortunately, *Figure 3* illustrates only the PE side of the 8hPB reinforced interface, as the PS peel arm had become separated prior to sectioning. However, it is clear that copolymer 8hPB forms lamellae at the interface. The period of these is approximately the same as measured in the bulk (i.e., 31.4 nm) [25]. *Figure 4* illustrates that the interfacial segregation behaviour of copolymer 101hPB is different to that of copolymer 8hPB. In this figure both the PS and PE homopolymer phases can be seen (the PE phase is darker (more heavily stained) with crystalline lamellae). What appears to be a monolayer of copolymer can be seen at the interface, with the remaining copolymer forming micelles in the PE phase.

The interfacial thickness and the organisation of the copolymer at the interface were also investigated by NR at the annealing temperature of 150°C using the melt cell

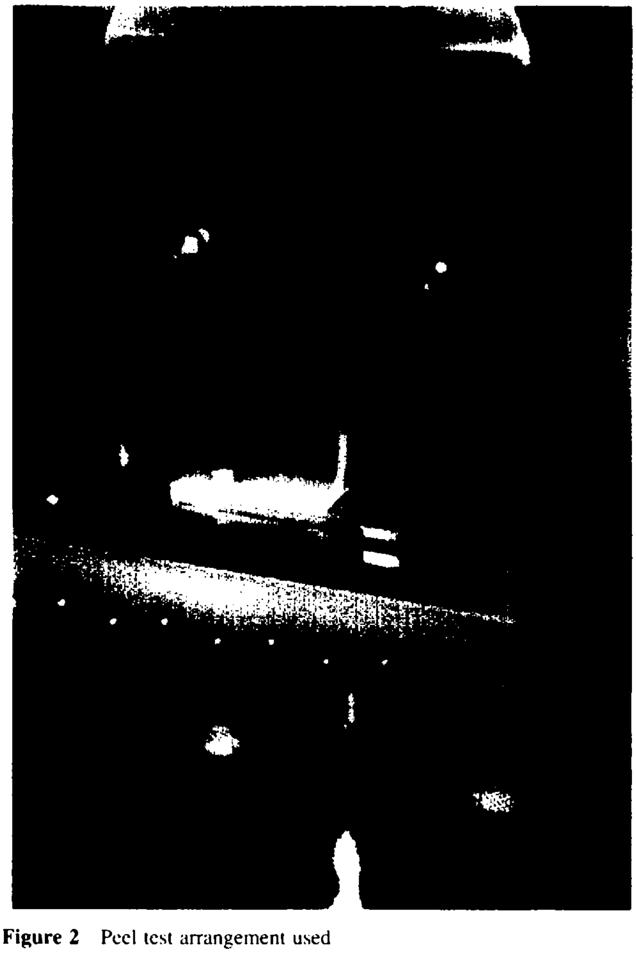

Figure 2 Peel test arrangement used

described above. *Figures 5 and 6* illustrate the data and corresponding scattering length density profile fits for the hPS/partially deuterated copolymer/PE samples with an original copolymer layer thickness of approximately 15 nm. The deuterated PS block of the copolymer has a much higher scattering length density than both the hydrogenous homopolymers and the hPB block of the copolymer, so its position at the interface can be clearly seen from the scattering length density profile fits. From these fits we can deduce that the interfacial roughness, σ, of the 10d8hPB-modified PS/PE interface is approximately 3.2 nm (i.e., it has an interfacial width (= $\sqrt{2\pi}\sigma$) of approximately 7.9 nm) and that the interfacial roughness of the 96d8hPB-modified PS/PE interface is approximately 7.7 nm (i.e., it has an interfacial width of approximately 19.3 nm). We have shown previously that the interfacial roughness of the unmodified PS/PE interface is 1.18 ± 0.33 nm (equivalent to an interfacial width of 2.96 ± 0.84 nm)[22]. These relatively modest increases in interfacial width are in agreement with those found by Russell and co-workers for interfaces which were not saturated with copolymer[3]. In the pure copolymer a higher molecular weight may be expected to result in a sharper interface. It is unclear why the reverse is observed for the copolymer-modified homopolymer interface.

The fit shown in *Figure 5* also indicates that the dPS block of copolymer 10d8hPB mixes to a depth of 4.4 nm with the PS homopolymer. The radius of gyration, R_g, of a PS chain of the same molecular weight as this block is 2.7 nm[27]. For a polymer chain with random conformation, the mean average end-to-end distance, L_{rc}, is $\sqrt{6}R_g$ i.e., for a polymer with this R_g, $L_{rc} \approx 6.6$ nm. Because one end of the dPS block of the copolymer is constrained to the PS/PE interface it will, in fact, form a brush and will not exhibit random conformation. The difference in molecular weights between the PS homopolymer and the PS-block of the copolymer may result in a certain degree of immiscibility and a 'dry' brush might be expected[28].

From the fit in *Figure 5* we can find the scattering length density of the dPS-block/hPS homopolymer mixed layer to be 5.05×10^{-6} Å^{-2}. From previous measurements[22], we have shown that the scattering length density of dPS at 150°C is 5.7×10^{-6} Å^{-2}. From this we can deduce that that of hPS at 150°C should be 1.35×10^{-6} Å^{-2} and hence from a simple balance we can calculate that the mixed layer must be composed of approximately 85% dPS. From this and knowing that the lamellar period of this copolymer in the bulk is 31.4 nm, we can calculate that the original copolymer layer was in fact 13.4 nm thick. This agrees well with the expected value of approximately 15 nm and provides a check on the model used to fit the data.

From *Figure 6* we can find in a similar manner to above, that the dPS-block of copolymer 96d8hPB mixes to a depth of 18.8 nm with the hPS homopolymer. This compares with an expected L_{rc} for this block of 20.8 nm. Also, that the mixed layer consists of approximately 33% dPS which corresponds to an original spun copolymer layer 12.8 nm thick. The values found for the original copolymer layer thickness for the two copolymers agree very well. Slight differences are always expected due to slight differences in solution concentration and spin speed. Unlike a 'free' chain with random conformation whose length is expected to scale

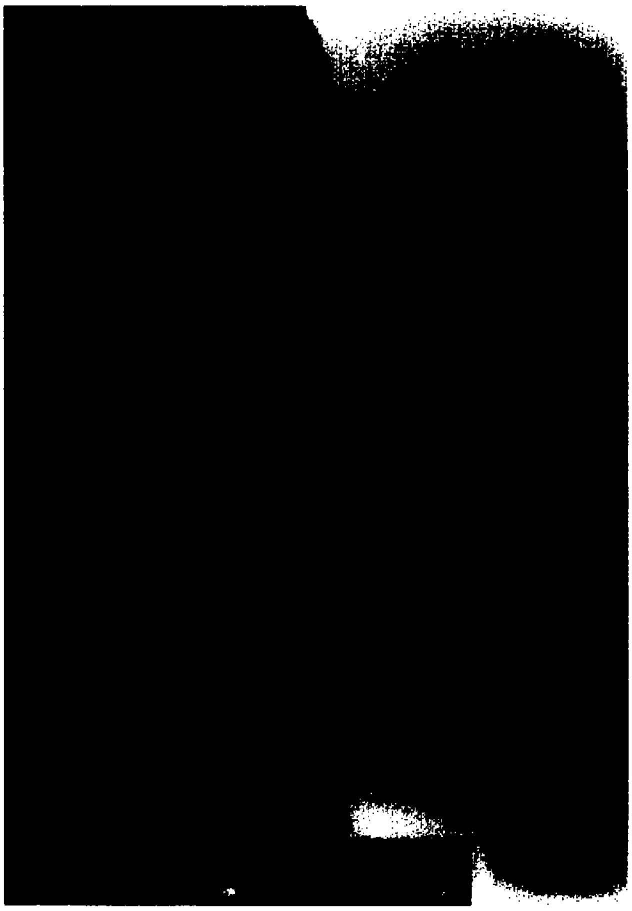

Figure 3 TEM micrograph of a PS/PE interface reinforced with a 60 nm thick 8hPB copolymer layer

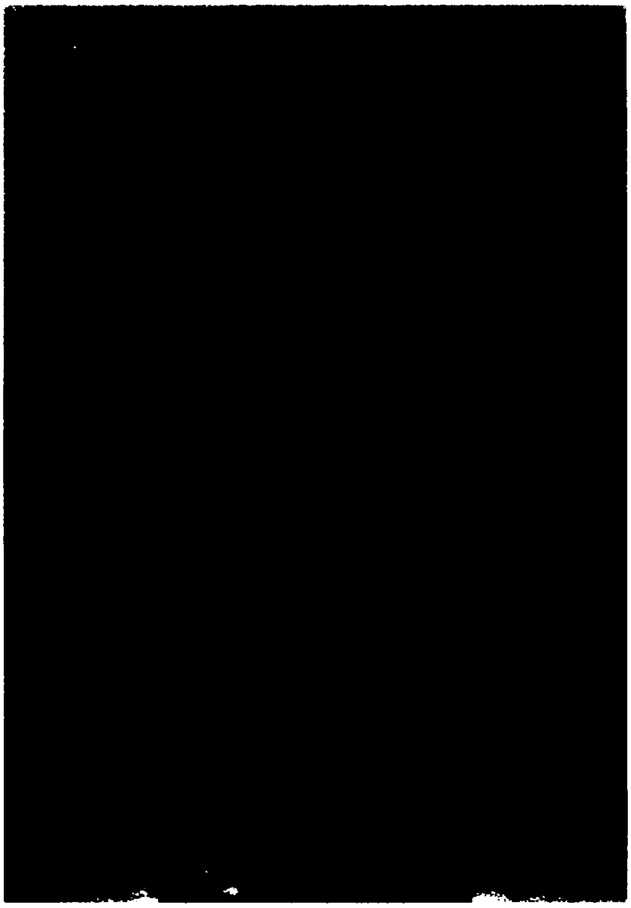

Figure 4 TEM micrograph of a PS/PE interface reinforced with a 60 nm thick 101hPB copolymer layer

with $\sqrt{N}$,the height, h, of a polymer brush (whether dry or wet) is reported[29] to scale with the degree of polymerisation, N, and the surface density, s, of the chains as follows: $h \propto Ns^{1/3}$. In these experiments a constant layer thickness of copolymer was placed at the interface. Thus, if the bulk density of the copolymer layer placed at the interface is assumed to be constant with molecular weight, s becomes inversely proportional to the molecular weight, M_w, of the

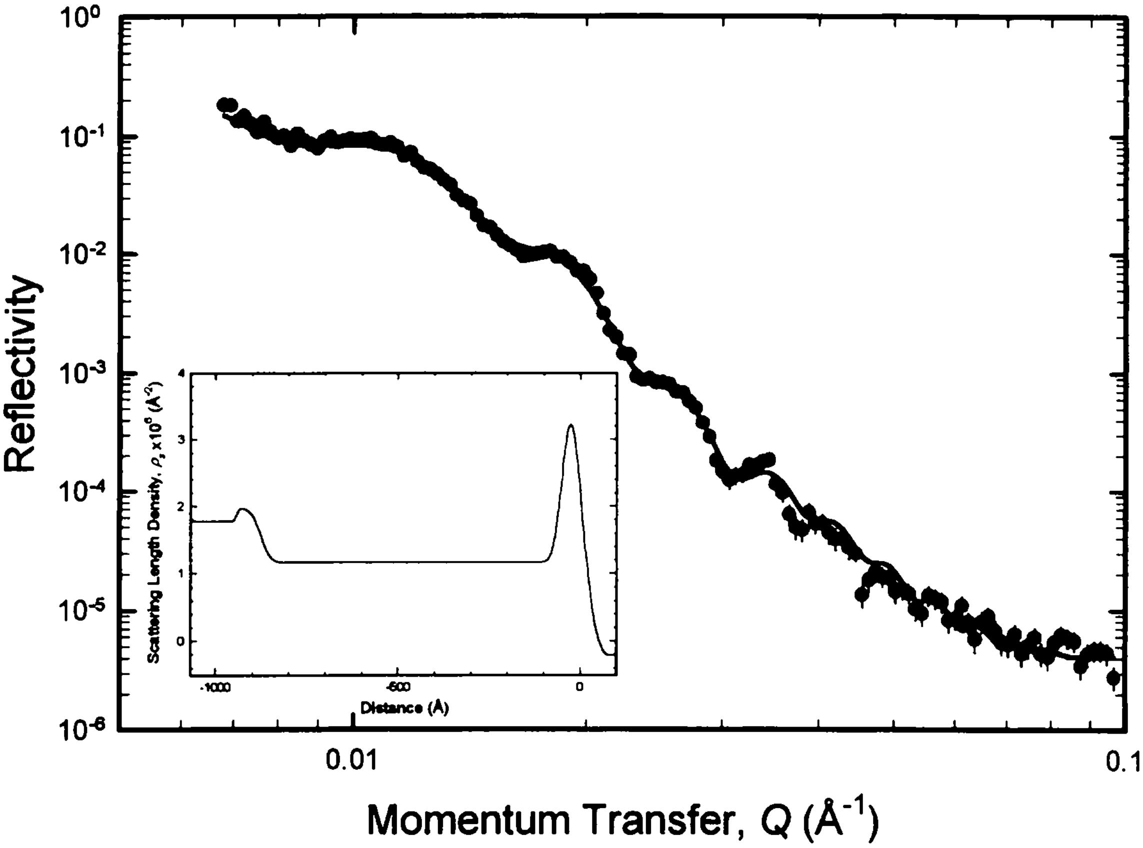

Figure 5 NR profile obtained at 150°C from a hydrogenous PS/PE interface modified by a 15 nm layer of the partially deuterated copolymer 10d8hPB. The fit (solid line) to the data (symbols) was obtained using the scattering length density profile shown in the inset

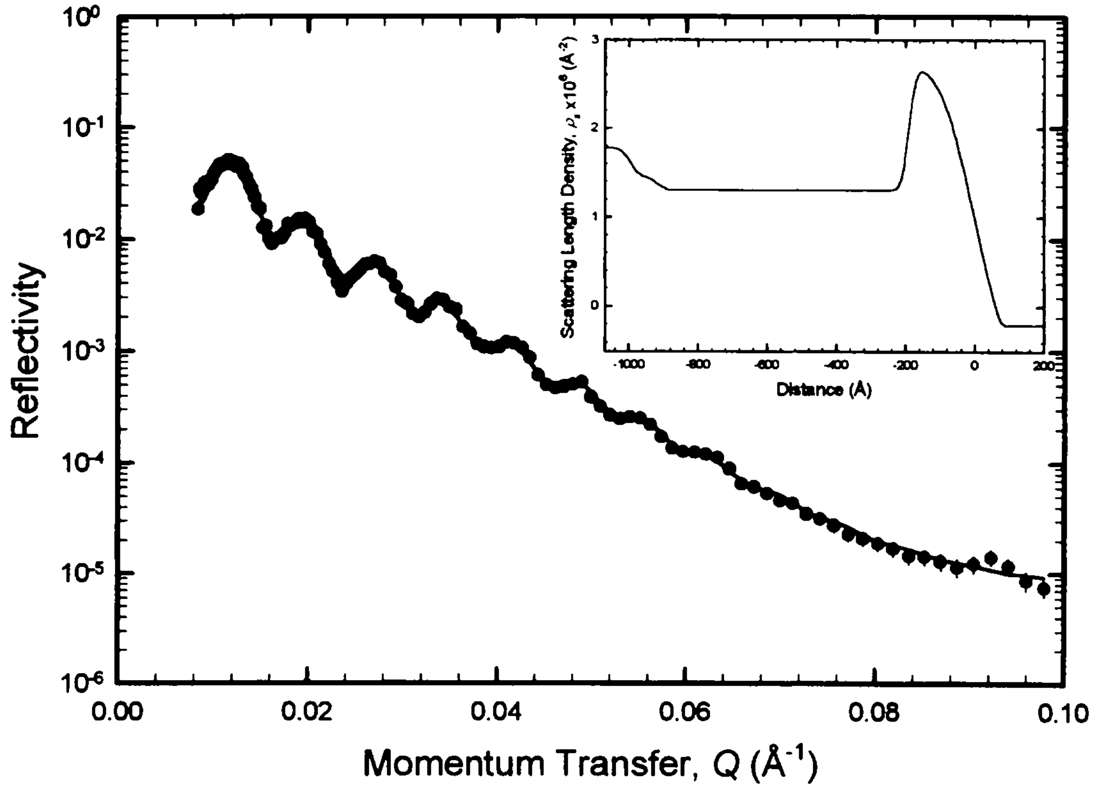

Figure 6 NR profile obtained at 150°C from a hydrogenous PS/PE interface modified by a 15 nm layer of the partially deuterated copolymer 96d8hPB. The fit (solid line) to the data (symbols) was obtained using the scattering length density profile shown in the inset

PS block forming the brush. As N is directly proportional to M_w, this results in the following relationship: $h \propto M_w^{2/3}$. Using the value of 4.4 nm obtained for the dPS 'brush' height of 10d8hPB and the molecular weights shown in *Table 2*, the height of the dPS brush formed by copolymer 96d8hPB at the PS/PE interface can be predicted to be 20.0 nm. This agrees surprisingly well with the value of 18.8 nm obtained from the fit to the data. If the slight differences in the original copolymer layer thickness are taken into account, the calculated values and those obtained from fitting the reflectivity profile agree even better.

A series of experiments using initial copolymer layer thicknesses of approximately 50 nm were also performed[25]. It was not possible to fit the data from these samples using the simple models described above and a layer which corresponded to a mixed copolymer layer had to be included in all the models. This mixed copolymer layer can be interpreted as micelles. However, because NR has no lateral resolution, the precise nature of this layer cannot be determined using this technique. In the case of the lower molecular weight copolymers, a mixed copolymer layer was sometimes found at the silicon interface. This was explained in terms of the lower surface energy of dPS compared with hPS being a stronger force than the miscibility of the hPB shells of the 'micelles' with the PE homopolymer. The multilayer structure observed in the TEM micrograph of the 8hPB-modified PS/PE interface illustrated in *Figure 3* was not seen in the NR profiles. The reason for this is unclear. However, the copolymer film placed between the PS and PE layers for the peel test specimen was approximately 60 nm thick, whereas that in the NR specimens was approximately 50 nm thick. If it is remembered that the average interdomain distance of the copolymer in the bulk is 31.4 nm, a possible explanation may be that the copolymer film in the peel test specimens is able to form complete layers, whereas that in the NR specimens is not and micelles are thus energetically more favourable.

A NR experiment was also performed to determine whether the copolymer must be placed at the PS/PE interface or whether it will migrate there of its own accord. A layer of a blend of dPS-homopolymer with 7.6 wt% 96d8hPB was spun onto a silicon block. This was placed against PE in the melt cell and the NR profile was measured at 150°C as for the samples described above. The resulting NR profile and the fit to the data were very similar to those for the PS/PE interface which had been reinforced with an approximately 50-nm layer of 96d8hPB. These results indicate that the copolymer does indeed have an affinity for the interface, and that the interface has attained equilibrium within the time required to align the melt cell in the NR beam (i.e., within an hour).

Interfacial strength

Figure 7 illustrates typical experimental traces obtained from two peel specimens with the same specimen configuration. The x-axis is the distance which the base plate has moved downwards. If no extension of the peel arm occurs, this is equal to the length of interface which has been peeled apart. The y-axis is the force recorded on the peel arm and is related to the interfacial strength of the specimen. As can be seen from *Figure 7*, curve (a) exhibits an initial peak. This is caused by the development of the peel arm i.e., the formation of the 90° bend and is a result of the elastic and plastic bending of the peel arm. Once the peel arm has developed and the interface starts to separate, the peel force can be seen to drop to a constant level. This drop is due to elastic recovery of the peel arm. Curve (b) does not exhibit this initial peak because during set-up of the experiment, the PS and PE slabs had been separated more than in case (a), such that the peel arm was already developed prior to measurement. After development of the peel arm, both curves have a similar shape: an initial approximately flat part from which the peel force is taken followed by an increase in the force. This increase is caused by the crack tip beginning to interact with the screw holding the sample in position. This interaction begins when the visible crack tip is still as much as 10 mm away from the screw.

The results from the peel tests are quoted as an average of the force obtained from the flat part of the curve for those specimens which exhibited a reasonable peel trace. Several sources of error were noted which might result in the measured force not being valid. The most dramatic of these was the effect of temperature. It was found that if the peel specimens were not stored in the constant temperature room overnight prior to testing, the measured peel force could be influenced significantly. For example, for one set of specimens an average peel force of approximately 3 N was found if the specimens had been held at 23°C for some time, whilst for a specimen which had been stored in an unheated laboratory (T ≈ 5°C at night) a peel force of approximately 8 N was measured. Another significant source of error arose from the sample preparation technique employed. Because each sample was prepared individually there was some overlap of the edge of the top layer. As may

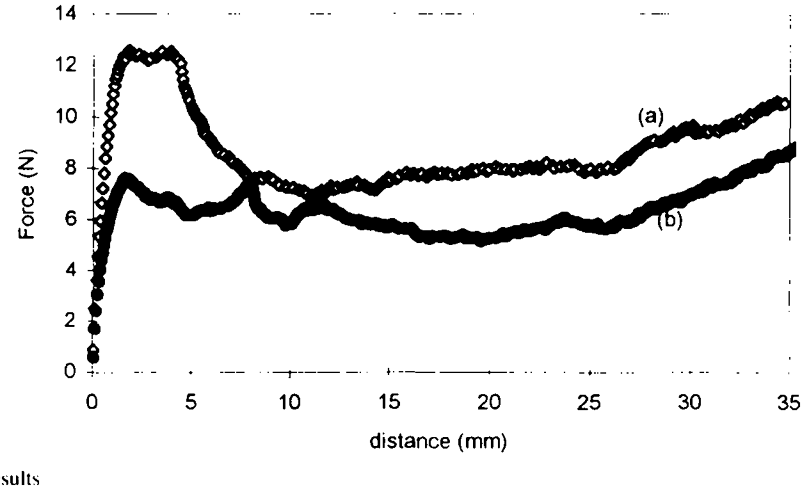

Figure 7 Typical peel test results

be imagined, this overlap led to a significant increase in the measured peel force. It was found that this problem could be remedied by carefully separating the overlap from the PS substrate at the edge of the sample using a scalpel. However, it is suggested that if similar experiments are performed in the future such edge effects might be avoided by preparing large 'sandwiches' from which the specimens can be carefully machined.

During peeling of some samples it was observed that the peel front did not always run perpendicular to the sides of the specimen and it was thought that this might result in false values for the peel strengths. Calculations showed, however, that even if a 20% increase in the width of the peel surface occurred, the change in peel force would still be within the expected error range. It had also been suggested that the toluene used to deposit the copolymer onto the PE may, in itself, improve the adhesion between the PS and PE layers. To check this, a sample was prepared in exactly the same manner as described above, but using pure toluene instead of the copolymer in toluene solution. It was found that the toluene had no effect on the interfacial adhesion i.e., as in the case where no copolymer is present, the act of removing the peel sandwich from the annealing mould was sufficient to separate the PE and PS slabs.

Measuring the interfacial strength between PS and PE without the addition of copolymer was not possible because, as mentioned above, removing the specimen from the annealing mould was sufficient to cause the two layers to separate. The very weak interface strength is associated with the small amount of interfacial diffusion, as indicated by the interfacial roughness, σ_{12}, of 1.18 ± 0.33 nm[22] measured at 150°C for the dPS/PE interface.

The effects of copolymer on the interfacial strength between PS and PE was investigated mainly using a fixed copolymer layer thickness. The results for the series of peel test specimens prepared using a constant copolymer film thickness of 15 nm and annealed for 100 min at 150°C are summarised in *Table 3*, and *Figure 8*. An immiscible homopolymer interface becomes saturated with copolymer when the thickness of the copolymer layer at the interface exceeds half the average interdomain distance, 0.5 L_0. For the copolymers 10d8hPB and 96d8hPB, L_0 has been shown to be 31.4 and 78.5 nm, respectively[25]. The values of L_0 for 8hPB and 101hPB are estimated to be approximately equal to those for 10d8hPB and 96d8hPB, respectively, owing to their similarity in molecular weights. Values of L_0 for 21hPB and 42hPB are approximated by interpolation from these values. Using these values of L_0 it is clear that only the 10d8hPB and 8hPB copolymers fully saturate the PS–PE interface $\Sigma \approx \Sigma_{sat}$.

Although the molecular weights of the hPB blocks of all the copolymers used are much greater than M_e(hPB) (≈ 2000), rubbery polymers above their T_g are relatively mobile and chain pullout may still occur relatively easily. At room temperature the hPB blocks of the copolymers and the PE homopolymer phase are above T_g but below T_m. Therefore, the copolymer will only be expected to be strongly anchored in the PE phase if co-crystallisation occurs. The DSC cooling curve of the grade of PE used[17] shows a sharp peak at 108°C associated with the crystallisation of the lightly branched chains and a weaker broad peak centred at 87°C associated with the crystallisation of the more highly branched chains[30]. These values can be compared with the crystallisation temperatures of the hPB blocks of the copolymers in *Table 4*. Co-crystallisation has been found only to occur when the temperature ranges over which crystallisation of the polymers occurs overlap and their crystal forms are comparable[31]. Although we have found using WAXS that the crystal structure of the hPB block of the copolymer is identical to that of polyethylene

Table 3 Summary of peel test results for a constant copolymer layer thickness of approximately 15 nm

Copolymer	8hPB	10d8hPB	21hPB	42hPB	96d8hPB	101hPB
M_w (PS)	8.2k	9.9k	21k	42k	96k	101k
M_w (hPB)	28.8k	16.7k	32.2k	80.9k	159.7k	113k
m (PS)	0.22	0.38	0.39	0.34	0.38	0.47
Peel force (N)	13.7	4.0	3.1	3.2	7.7	7.8

Table 4 Crystallisation and melting temperatures of the hPB blocks of the copolymers

Copolymer	8hPB	21hPB	42hPB	101hPB	10d8hPB	96d8hPB
T_m (°C)	95	99	94	92	96	95
$T_{cryst.}$ (°C)	77	78	74	74		73
	68	68			67	
	58	58	54[a]		55	54

[a] Very small compared with major peak

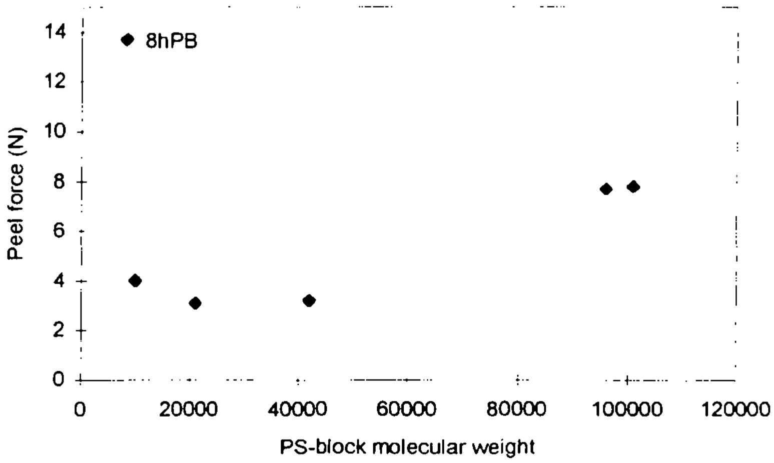

Figure 8 Measured peel force as a function of PS-block molecular weight for a constant copolymer layer thickness of approximately 15 nm

(i.e., orthorhombic) (R. L. Scherrenberg, unpublished), because of the differences in crystallisation behaviour observed using DSC we cannot be certain whether cocrystallisation occurs.

The molecular weights of the PS-blocks of the copolymers varied from approximately $0.5M_c$ to approximately $5M_c$ (M_c(PS) ≈ 20000). For the short PS-blocks ($M_w < M_c$) chain pullout from the PS homopolymer phase is expected to occur relatively easily. By contrast, when $M_w > M_c$ the PS-block of the copolymer is expected to be strongly anchored in the homopolymer phase. For a constant volume of copolymer the relative number of copolymer chains is inversely proportional to the molecular weight of the copolymer assuming constant density. Assuming that all the copolymer chains are at the interface, the relative areal densities can be estimated from the inverse of the copolymer molecular weight. *Table 5* summarises the predictions of change in interfacial strength with copolymer molecular weight for a copolymer layer thinner than 0.5 L_0 (i.e., $\Sigma < \Sigma_{sat}$) assuming that the hPB blocks of the copolymer are well anchored within the PE homopolymer phase. These predictions show that the interfacial strength of the 8hPB and 10d8hPB modified interfaces should be similar and quite low, the strength of the 96d8hPB and 101hPB modified interfaces should be higher and the strength of the 21hPB and 42hPB modified interfaces intermediate between these extremes. Scaling the peel force by the relative number of copolymer chains (N from *Table 5*), the interfacial strength as a function of block copolymer molecular weight as shown in *Figure 9* is obtained. The values of interfacial strength obtained agree reasonably well with the trend in *Table 5*. This indicates that the pullout behaviour of the PS block of the copolymer from the PS homopolymer phase dominates the fracture behaviour of the interface.

The difference in peel strength observed for the 8hPB and 10d8hPB reinforced interfaces suggest, however, that not only the molecular weight of the PS-block of the copolymer determines the strength of the interface. From the similarities in the peel curves for the 96d8hPB and 101hPB-reinforced interfaces (not shown) it can be deduced that, for this system, deuteration of the PS-block of the copolymer has no significant effect on the interfacial strength of the interface. From *Table 3*, copolymer 8hPB can be seen to be more asymmetric and to have a much higher molecular weight hPB-block than copolymer 10d8hPB. If there is little or no co-crystallisation between the hPB blocks of the copolymer and the PE homopolymer, the energy required to pull the hPB-block out of the PE will depend upon the length of the hPB-block. The hPB-block of copolymer 10d8hPB may be expected to pull out of the PE much more easily that that of copolymer 8hPB. The large difference in peel force measured for these two interfaces may therefore be explained as follows: at the 10d8hPB reinforced interface, neither the hPB nor the PS-block of the copolymer are well anchored within their respective homopolymers. Due to its lower friction coefficient, the hPB is pulled out of the PE phase during the peel test. At the 8hPB reinforced interface, by contrast, the hPB-block is better anchored in the PE phase due to its much longer length, so that the PS-block of the copolymer is pulled out of the PS homopolymer during peeling. This requires more energy than pulling out a short hPB block and the measured peel force is therefore higher. This explanation is backed up by preliminary XPS results which suggested that the surface of the PS peel arm resulting from the 10d8hPB reinforced interface was partially covered with hPB, whilst that resulting from the high molecular weight 96d8hPB reinforced interface indicated no hPB on the PS peel arm within the limit of detection (approximately 10%)[25].

Increasing the thickness of the copolymer layer at the PS/PE interface to approximately 60 nm increased the mea-

Table 5 Prediction of the trend in interfacial strength with copolymer molecular weight for copolymer layers thinner than 0.5 L_0 (assuming that the hPB block of the copolymers are well anchored)

Copolymer	8hPB	10d8hPB	21hPB	42hPB	96d8hPB	101hPB
M_w (PS)	8.2k	9.9k	21k	42k	96k	101k
M_w (total)	37k	26.6k	54.2k	122.9k	255.7k	214k
Regime	III		II		I	
Expected behaviour	chain pullout strength ∝ Σ		pullout or crazing depending on Σ		chain scission strength ∝ Σ^2	
$N = 1/(M_w(\text{total})) \propto \Sigma$	$2.7e^{-5}$	$3.6e^{-5}$	$1.8e^{-5}$	$0.8e^{-5}$	$0.4e^{-5}$	$0.5e^{-5}$
Rank in interfacial strength (1 = weakest)	1	2	depends upon whether $\Sigma < \Sigma^*$		5	6

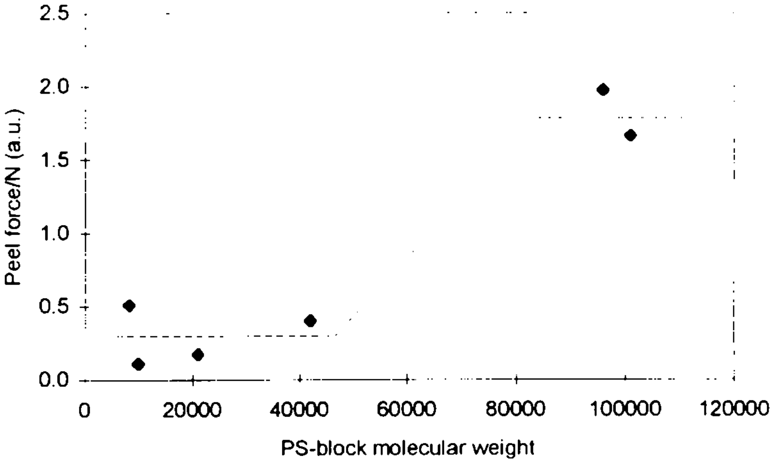

Figure 9 Measured peel force scaled by the number of chains at the interface as a function of PS-block molecular weight for a constant copolymer layer thickness of approximately 15 nm

sured peel force for copolymer 8hPB from 13.7 to 23.6 N. For copolymer 101hPB at a similar thickness, the adhesion between the PS and PE was sufficient to prevent the homopolymer layers from separating in the peel test. The PE arm yielded and broke before any indication of peeling was visible. This indicates that the peel force necessary to separate the two layers exceeds the yield point of PE, which is approximately 140 N. Such a large increase in peel strength has to our knowledge not previously been reported in the literature. From the work on amorphous copolymers by Washiyama and co-workers, it is expected that the formation of multiple layers leads to a reduction in peel strength for the case where lamellae are formed, or no change in peel strength if cylinders are formed at the interface [11]. In the TEM micrographs discussed in the previous section, it was shown that for this layer thickness, copolymer 8hPB forms multiple layers at the interface and copolymer 101hPB forms micelles or cylinders. The unexpectedly high interfacial strengths observed in these investigations may be a consequence of the semi-crystallinity of the hPB blocks of the copolymers and of the PE homopolymer.

Reducing the annealing time from 100 to 10 min was found to have only a small effect on the strength of the PS/PE interface modified by a 15 nm copolymer layer. For copolymer 101hPB the peel force decreased from 7.8 N for 100 min annealing time to 6.9 N for 10 min. For 8hPB the peel force dropped from 13.7 to 9.0 N for the same annealing times, respectively. This could suggest one of two extremes. Firstly, that the copolymers attain their equilibrium conformations very quickly or, secondly, that equilibrium has not been attained after 100 min. For high molecular weight copolymers, Brown and co-workers report that an annealing time of 2 h was insufficient to enable thick films to organise completely[9]. However, from NR experiments we have found evidence that these interfaces reach equilibrium after an hour of annealing. Further experiments are required to resolve these two hypotheses.

CONCLUSIONS

It has been shown that the semi-crystalline PS-b-hPB copolymers investigated segregate to the interface between PS and PE, where the blocks of the copolymer penetrate into the respective homopolymer phases. The penetration depth of the PS block of the copolymer into the homopolymer was found to scale with molecular weight according to theories describing polymer brush behaviour.

Presumably as a result of the penetration of the copolymer blocks into the respective homopolymers, the PS-b-hPB copolymers were found to increase the strength of the interface between PS and PE. Evidence that both the hPB and PS blocks may pull out of the respective homopolymer phases was found. However, the trend in interfacial strength was found to be dominated by the molecular weight of the PS block of the copolymer.

Once the interface between the PS and PE became saturated with copolymer, addition of further copolymer resulted in the formation of micelles or multilayer structures at the interface. In contrast to results in the literature for amorphous systems, these micelles/structures were not found to result in a reduction in the interfacial strength compared with that obtained when a monolayer of copolymer was present at the interface. The high molecular weight copolymer reinforced interface, in fact, became so strong that it could not be separated. From NR measurements it is believed that the annealing time was sufficient to allow the interface to attain its equilibrium conformation. Hence, it is not believed that these strong interfaces are a consequence of a non-equilibrium morphology at the interface.

ACKNOWLEDGEMENTS

The funding of this research by EPSRC, UK and DSM Research, The Netherlands in the form of a CASE studentship is gratefully acknowledged. The copolymers were synthesised by Lizette Schmieder, the TEM micrographs were prepared by Monique Walet, DSM Research and the peel tests were performed with the help of Sarah Holton and Tony Kinloch, Department of Mechanical Engineering, Imperial College.

REFERENCES

1. Hermes, H. E. and Higgins, J. S., *Poly. Eng. Sci.*, in press.
2. Shull, K. R. and Kramer, E. J., *Macromolecules*, 1990, **23**, 4769.
3. Russell, T. P., Menelle, A., Hamilton, W. A., Smith, G. S., Satija, S. K. and Majkrzak, C. F., *Macromolecules*, 1991, **24**, 5721.
4. Brown, H. R., *Macromolecules*, 1989, **22**, 2859.
5. Cho, K., Brown, H. R. and Miller, D. C., *J. Poly. Sci.: Part B: Poly. Phys.*, 1990, **28**, 1699.
6. Creton, C., Kramer, E. J. and Hadziioannou, G., *Macromolecules*, 1990, **24**, 1846.
7. Creton, C., Kramer, E. J., Hui, C.-Y. and Brown, H. R., *Macromolecules*, 1992, **25**, 3075.
8. Washiyama, J., Kramer, E. J. and Hui, C.-Y., *Macromolecules*, 1993, **26**, 2928.
9. Brown, H. R., Char, K., Deline, V. R. and Green, P. F., *Macromolecules*, 1993, **26**, 4155.
10. Char, K., Brown, H. R. and Deline, V. R., *Macromolecules*, 1993, **26**, 4164.
11. Washiyama, J., Creton, C., Kramer, E. J., Xiao, F. and Hui, C.-Y., *Macromolecules*, 1993, **26**, 6011.
12. Creton, C., Brown, H. R. and Deline, V. R., *Macromolecules*, 1994, **27**, 1774.
13. Washiyama, J., Kramer, E. J., Creton, C. F. and Hui, C.-Y., *Macromolecules*, 1994, **27**, 2019.
14. Reichert, W. F. and Brown, H. R., *Polymer*, 1993, **34**(11), 2289.
15. Brown, H. R., *Macromolecules*, 1993, **26**, 1666.
16. Creton, C., Brown, H. R. and Shull, K. R., *Macromolecules*, 1994, **27**, 3174.
17. Deblieck, R. A. C. and Mathot, V. B. F., *J. Mat. Sci. Letters*, 1988, **7**, 1276.
18. Stamm, M., *Adv. Poly. Sci.*, 1992, **100**, 357.
19. Stamm, M., *J. Appl. Cryst.*, 1991, **24**, 651.
20. Bucknall, D. G. and Higgins, J. S., in *Recent Developments in Polymer Science*, ed. H. Hommel, 1997. Reprinted as RAL report RAL-TR-97-008: T. P. Russell, Mat. Sci. Reports 1990, **5**, 171.
21. Higgins, J. S. and Oiarzabal, L., ISIS Annual Report, 1993, RB4116, A156.
22. Hermes, H. E., Bucknall, D. G. and Higgins, J. S., *Polymer*, 1997, **38**(4), 985.
23. Heavens, O. S., *Optical Properties of Thin Films*, Butterworth, London, 1955.
24. Sivia, D. S., Hamilton, W. A. and Smith, G. S., *Physica B*, 1991, **173**, 121.
25. Hermes, H. E., Bulk and interfacial properties of compatibilised polymer blends. PhD thesis, University of London, 1996.
26. Kinloch, A. J., Lau, C. C. and Williams, J. G., *Int. J. Fracture*, 1994, **66**, 45.
27. Brandrup, J. and Immergut, E. H. (ed.), *Polymer Handbook*, 3rd edn. Wiley Interscience, New York, 1989.
28. Tanaka, H., Hasegawa, H. and Hashimoto, T., *Macromolecules*, 1991, **24**, 240.
29. Milner, S. T., *Science*, 1991, **251**, 905.
30. Mathot, V. B. F., Proceedings POLYCON '84-LLDPE, The Plastics and Rubber Institute and The Society of Plastics Engineers, 1984.
31. Nadkarni, V. M. and Jog, J. P., in *Two Phase Polymer Systems*, ed. L. A. Utracki, Hanser, Munia, 1991.